




Regeneration of pulp-dentin complex using human stem cells of the apical papilla: *in vivo* interaction with two bioactive materials

Diana B. Sequeira^{1,2} · Ana Rafaela Oliveira^{1,3} · Catarina M. Seabra^{1,4} · Paulo J. Palma² · Carlos Ramos^{5,6} · Maria H. Figueiredo² · Ana C. Santos^{5,6} · Ana L. Cardoso^{1,4} · João Peça^{1,7} · João Miguel Santos^{2,4} 

Received: 16 December 2020 / Accepted: 15 February 2021 / Published online: 25 February 2021
© Springer-Verlag GmbH Germany, part of Springer Nature 2021

Abstract

Objectives To compare the regenerative properties of human stem cells of the apical papilla (SCAPs) embedded in a platelet-rich plasma (PRP) scaffold, when implanted *in vivo* using an organotypic model composed of human root segments, with or without the presence of the bioactive cements – ProRoot MTA or Biodentine.

Material and methods SCAPs were isolated from third molars with incomplete rhizogenesis and expanded and characterized *in vitro* using stem cell and surface markers. The pluripotency of these cells was also assessed using adipogenic, chondrogenic, and osteogenic differentiation protocols. SCAPs together with a scaffold of PRP were added to the root segment lumen and the organotypic model implanted on the dorsal region of immunodeficient rats for a period of 4 months.

Results Presence of SCAPs induced *de novo* formation of dentin-like and pulp-like tissue. A barrier of either ProRoot MTA or Biodentine did not significantly affect the fraction of sections from roots segments observed to contain deposition of hard material ($P > 0.05$). However, the area of newly deposited dentin was significantly greater in segments containing a barrier of Biodentine compared with ProRoot MTA ($P < 0.001$).

Conclusions and clinical relevance SCAPs offer a viable alternative to other dental stem cells (DSCs) in their regenerative properties when enclosed in the microenvironment of human tooth roots. The present study also suggests that the presence of bioactive materials does not hinder or impede the formation of new hard tissues, but the presence of Biodentine may promote greater mineralized tissue deposition.

Keywords Cell differentiation · Endodontics · Regeneration · Regenerative endodontics · Stem cells · Stem cells from the apical papilla

✉ João Miguel Santos
jsantos@fmed.uc.pt

¹ CNC - Center for Neuroscience and Cell Biology, University of Coimbra, Coimbra, Portugal

² Institute of Endodontics, Faculty of Medicine, University of Coimbra, Coimbra, Portugal

³ MIT Portugal PhD Program, Universidade Nova de Lisboa, Lisbon, Portugal

⁴ Institute for Interdisciplinary Research, University of Coimbra, Coimbra, Portugal

⁵ Coimbra Institute for Clinical and Biomedical Research (iCIBR) – CIBB, University of Coimbra, Coimbra, Portugal

⁶ Institute of Biophysics, Faculty of Medicine, University of Coimbra, Coimbra, Portugal

⁷ Department of Life Sciences, University of Coimbra, Coimbra, Portugal

Introduction

Regenerative medicine and tissue engineering are critically intertwined with advances in stem cell biology. Since the discovery of bone marrow mesenchymal stem cells [1], additional tissues have been identified to contain niches of multipotent stem cells. Notably, these include epidermal stem cells present in hair follicles, epithelial stem cells in the intestine, or neural stem cells in the subventricular zone of the brain [2, 3]. In 2000, Gronthos et al. isolated and characterized a population of human dental pulp stem cells (DPSCs) [4]. Subsequent studies isolated and characterized additional human dental stem cells (hDSCs) populations, such as stem cells from exfoliated deciduous teeth (SHED) [5], stem cells from periodontal ligament tissue (PDLSCs) [6], dental follicle precursor cells (DFPCs) [7], and stem cells from the apical papilla (SCAPs) [8, 9].

During development, teeth are formed from reciprocal interactions between ectoderm-derived epithelial cells and neural crest cells [10]. In turn, adult dental stem cells display broad multidifferentiation potential *in vitro*, having been demonstrated to differentiate into odontoblasts, adipocytes, chondrocytes, osteoblasts, and neuronal populations [10–13]. Several studies have assessed how hDSCs and their conditioned media may aid regenerative medicine, both in dentistry and in broader branches of medicine [14]. Some examples include the use of SHED or DPSCs to improve the outcome in animal models of Alzheimer's disease or stroke [15, 16], cardiac repair [17], or autoimmune disorder [18]. DSCs showed potential in dental pulp revascularization [19] and regenerative endodontic therapy [20]. DPSCs transplanted *in vivo* with hydroxyapatite/tricalcium phosphate produced dentin [21], while SHEDs seeded in biodegradable scaffolds have also demonstrated similar potential for *in vivo* applications [22, 23]. Recently, the first clinical application of DPSCs from deciduous teeth and mobilized DPSCs have been performed [24, 25]. These seminal studies showed the regeneration of pulp tissue [24, 25] and the presence of blood vessels and sensory nerves in human patient using autologous transplants [25]. While human trials have focused so far on DPSCs, recent evidence also suggest SCAPs may display similar potential for the deposition of pulp-like tissue [26] and may even be recruited in regenerative endodontic procedures in immature teeth [27].

Endodontic regenerative treatments apply the tissue engineering triad of cells, scaffold, and growth factors to regenerate the dentin and pulp tissues. Platelet-rich plasma (PRP) has been used as a natural bioactive scaffold in dentistry for several years, with several *in vivo* and case series studies published in the literature [28–30]. PRP contains growth factors including endothelial growth factor (VEGF), transforming growth factor- β (TGF- β), fibroblast growth factor (FGF), and platelet-derived growth factor (PDGF) that play an important role in tissue repair/regeneration [29]. During recent years, PRP gained special interest on regenerative endodontics, especially on pulpotomy, apexification, and apical surgery, being considered as a potential ideal scaffold in this field [31]. Autologous PRP acts as ideal natural biodegradable three-dimensional scaffold, supporting cell growth and differentiation, and releases several growth factors that influence tissue regeneration [32]. However, to date no studies have assessed the potential of using PRP as a scaffold for SCAPs in regenerative procedures.

Comparative studies assessing the interaction of different dental stem cell populations with commonly used bioactive materials require further exploration in order to maximize potential regeneration in the clinical setting. For example, we have recently assessed the differential responses in cell proliferation and viability of SCAPs exposed to compounds commonly used in the clinical setting [33]. As the application of

hDSCs expands, it is necessary to determine which compounds may present more favorable characteristics when performing human pulp-dentin complex regeneration procedures *in vivo*.

New bioactive materials with regenerative capacities should promote stem cell differentiation without diminishing self-proliferation, while at the same time displaying good biocompatibility. Mineral trioxide aggregate (ProRoot® MTA, Tulsa Dental, Johnson City, TN, USA) is the most common biomaterial used in endodontic treatment, including in apexogenesis, apexification, perforation repair, pulpotomy, apical filling, and root resorptions. The success of this biomaterial is due to its optimal biocompatibility, low cytotoxicity, antimicrobial activity, sealing ability, high pH, low solubility, hydrophilicity, radiopacity, and setting expansion. In regenerative procedures, several studies have revealed that MTA can induce stem cell proliferation and differentiation from dental pulp, germs, periodontal ligament tissue, and stem cells from apical papilla [34–37]. In 2009, a new tricalcium-silicate cement, Biodentine (Biodentine™, Septodont, Saint-Maur-des-Fossés, France) became available. Comparing Biodentine to MTA, this new tricalcium cement presents similar biological properties to MTA but is more cost-effective and technically easier to handle (has a better consistency), has faster setting time, and contains zirconium oxide as radiopacifier [38], allowing a lower potential of tooth discoloration [38, 39].

The present work aimed to highlight the pulp-dentin complex regenerative ability of SCAPs and to perform a comparison of ProRoot MTA and Biodentine, as potential materials for application with SCAPs in regenerative endodontic procedures, using PRP as a bioactive scaffold. Our null hypothesis was that both materials display similar properties in terms of facilitating tissue regeneration *in vivo*, when applied together with SCAPs in human tooth roots. To assess the performance of both compounds, we characterized human SCAPs, cultured these cells, and applied them with a platelet-rich plasma (PRP) scaffold into human root segments as an organotypic model. Root segments with or without a biomaterial barrier were implanted in immunodeficient rats for a four-month period before histological analysis.

Materials and methods

Biomaterials used

The endodontic biomaterials tested in this investigation were White ProRoot MTA and Biodentine. Their composition, as supplied by the manufacturers, is presented in Table 1.

Tooth collection and cell culture

Third molars with incomplete rhizogenesis were collected from 3 donors presenting orthodontic indication for

Table 1 Composition of tested biomaterials

Materials and Manufacturer	Component A	Component B
White ProRoot® MTA Dentsply Tulsa Dental, Johnson City, TN, USA	Powder: calcium phosphate, calcium oxide, silica, bismuth oxide	Liquid: distilled water
Biodentine™ Septodont, Saint-Maur-des-Fossés, France	Powder: tricalcium silicate, dicalcium silicate, calcium carbonate, calcium oxide, iron oxide, zirconium oxide	Liquid: water with calcium chloride, hydro soluble polymer (polycarboxylate)

extraction. Informed consent was obtained from all participants, according to the approval of the Ethics Committee of the Faculty of Medicine, University of Coimbra (Project CE-028/2016), and following the guidelines of the Declaration of Helsinki. Upon dental extraction, human gingiva was collected and apical papillae were gently detached from the apical foramen of the root and minced into small portions, as previously described [33, 40].

Isolation and culture of human apical papillae cells

Apical tissues were enzymatically digested with type I collagenase (3 mg/mL) and dispase (4 mg/mL) for 1 hour, at 37 °C. The suspension was gently mixed every 15 min to facilitate dissociation of the tissue. To obtain single cell suspensions, the solution was resuspended and passed through a 70 µm cell strainer, followed by centrifugation at 300 g, for 5 min, at room temperature. Cell pellet was then resuspended and cultured in SCAPs medium composed of Knock Out-Dulbecco Modified Eagle Medium (KO-DMEM) (Gibco, Alfacene), supplemented with 20% FBS, 100 units/mL penicillin (Gibco, Invitrogene), 100 mg/mL streptomycin (Gibco, Invitrogene), GlutaMax (Gibco, Invitrogene) and β-mercaptoethanol (EmbryoMax, Merck Millipore), and incubated at 37 °C with 5% CO₂. Cells were cultured to 80% confluency and passaged at a 1:3 ratio. Cells at passages 5–8 were used for all experiments described below.

Isolation and culture of human gingival fibroblasts

The epithelial layer of the gingival tissue was removed under magnification, and the connective tissue was minced into small pieces and enzymatically digested, as described above. Fibroblast cultures were maintained in Knock Out-Dulbecco Modified Eagle Medium (KO-DMEM) (Gibco, Alfacene), supplemented with 20% FBS, 100 units/mL penicillin (Gibco, Invitrogene), 100 mg/mL streptomycin (Gibco, Invitrogene), GlutaMax (Gibco, Invitrogene) and β-mercaptoethanol (EmbryoMax, Merck Millipore), and incubated at 37 °C with 5 % CO₂. Cells were cultured to 80% confluency and passaged at a 1:3 ratio. Cells at passages 5–8 were used for all experiments.

Immunohistochemistry

To determine if the newly formed tissues in the implanted roots were from rat or human origin, an antibody against human mitochondria was used (MAB1213, Merck, Millipore). Root sections (see below) were deparaffinized and rehydrated. To perform deparaffinization, sections were placed twice in xylene for 3 min each. Then, to rehydrate, slides were transferred to 100% alcohol, for two changes, 3 min each, and then transferred once through 96 and 70% alcohols, 3 min each. To complete rehydration, sections were rinsed with PBS two times, 5 min each. Antigen retrieval was performed using a citrate buffer, pH 6.0. Slides were placed in a staining container with citrate buffer and incubated at 85 °C for 20 min. After this period, the staining container was removed, and the buffer replaced with fresh buffer at room temperature. Samples were then allowed to cool for 20 min and rinsed with PBS, permeabilized with 0.025% Triton in PBS and blocked for 2 h with a solution of 10% normal goat serum, 1% BSA in PBS. Diluted primary antibody (1:1000 anti-mitochondria antibody MAB1213, Merck, Millipore) was added and sections incubated overnight at room temperature. Primary antibody solution was removed, and slides washed with PBS. The secondary antibody was applied at a dilution of 1:200 (A-11001, Molecular Probes, Invitrogen) and incubated for 2 h at room temperature. Secondary antibody solution was removed, and slides washed three times with PBS and section mounted with VectaShield HardSet (H-1500, Vector Laboratories). Images were acquired using a Confocal LSM 710 Carl Zeiss microscope, a Plan-Apochromat 40x/1.4 Oil lens, and processed using Zen Software (Zeiss).

In vitro differentiation of SCAPs

The ability to differentiate into different tissue types was used to validate multipotential of SCAPs cultures. For this, SCAPs were plated onto 6-well plates and exposed to three independent solutions for: i) adipogenic differentiation (STEMPRO® Adipogenesis Differentiation Kit, Gibco), ii) osteogenic differentiation (STEMPRO® Osteogenesis Differentiation Kit, Gibco), iii) chondrogenic differentiation (STEMPRO® Chondrogenesis Differentiation Kit, Gibco). After two weeks in culture, the cells were rinsed once with PBS and fixed with

4% PFA solution for 30 min. Cells were then processed using staining procedure specific for each lineage, specifically: Oil Red O for adipocytes, Alcian Blue for chondrocytes and Alizarin Red S for osteocytes. Stained cells were then visualized using a light microscope for a qualitative analysis.

Flow cytometry

To determine proteins expressed on their surface, SCAPs were analyzed by flow cytometry. The following surface markers were analyzed: CD14 (Sigma SAB4700106-100TST), CD24 (Biolegend 311,103), CD105 (Biolegend 323,203), CD45 (Biolegend 368,509), CD146 (Biolegend 361005), CD44 (Abcam ab95514), STRO-1 (Biolegend 340103), and CD73 (Biolegend 344005) following manufacturer's instructions. Briefly, SCAPs were rinsed once with PBS containing 10% of fetal bovine serum (PBS/10% FBS) and then incubated for 30 min at 4 °C in the dark with each antibody in a solution of PBS with 3% of bovine serum albumin (BSA). After this period, cells were washed once with PBS/10% FBS and twice with PBS. Lastly, cells were resuspended in 200 to 300 µL of PBS. 7-amino-actinomycin D (7-AAD, Sigma) (50 µg/mL) was added 5 min before analysis as an indicator of cell viability. Unstained cells were used as controls. All flow cytometry acquisitions were made using a FACSCalibur flow cytometer (BD Biosciences, USA), and a total of 10,000–20,000 events were collected in the established gate for each condition.

Organotypic model

Adult human teeth with indication for extraction for orthodontic reasons were collected, and periodontal tissues were removed from the root surface with a sterile periodontal curette. Teeth were stored in PBS supplemented with 100 U/mL penicillin, 100 U/mL streptomycin, and Fungizone to prevent contamination. Teeth were then washed three times with PBS. Crown regions were removed, and radicular portions were horizontally sectioned with a low-speed saw into 6 mm segments in length. The root canal spaces were prepared with a diameter of 1–1.5 mm using a sequence of Gates Glidden burs (number 1,2,3 and 4). Root segments were then first soaked in 6% NaOCl (CanalPro™ 6% NaOCl, Coltène/Whaledent, Altstätten, Switzerland) 1 min; afterwards, root canals were irrigated with 3% NaOCl (CanalPro™ 3% NaOCl) (20 mL/3 min) at room temperature and then rinsed with 17% EDTA (CanalPro™ EDTA) (5 mL/1 min) and saline solution (0.9% NaCl) (10 mL/5 min) to remove smear-layer. Roots were again rinsed 3 times with sterile PBS. Roots were then randomly assigned to one of the four experimental groups and those designated to receive a biomaterial (ProRoot MTA or Biodentine) were further processed to receive an apical barrier. The biomaterials barriers were prepared

according to manufacturer's instructions immediately before filling the root implants with SCAPs and PRP.

Platelet-rich plasma and SCAPs

SCAPs from a single donor were expanded in culture and harvested on the day of the procedure. To prepare platelet-rich plasma (PRP), blood from a single donor was collected on the same day, into a sodium citrate solution (3.8% w/v) and centrifuged at 620 g for 8 min, to obtain PRP and platelet-poor plasma (PPP) without erythrocytes and leukocytes. The top layer (PRP + PPP) was then again centrifuged at 3200 g for 12 min. Top layer was removed, and the bottom 1 mL was harvested as PRP. SCAPs were added to fresh PRP at a final concentration of 1×10^6 cells/mL. To trigger fibrin polymerization and initiate PRP coagulation, 0.025 M calcium chloride was added. The PRP/SCAPs cell suspension was then injected into the canal space to the level of the cemento-enamel junction and allowed at least 3 min to complete clot formation before surgical implantation. In roots that did not contain a barrier, a cushion of Parafilm M (Amcor, Zürich, Switzerland) was used to firmly press the root segment, temporarily sealing the corresponding extremity, until PRP coagulation was achieved.

Subcutaneous implantation

Root segments with or without cellular clot were kept in 24 well plates with minimum quantity of cell culture media. For the *in vivo* assay, seventeen 8–10 weeks female immunodeficient (RNU) rats were used. Animals were housed in a temperature-controlled room under 12:12 h day/night cycle, with food and water provided ad libitum. All procedures were performed in accordance with European Communities Council Directive of 24 November 1986 (86/609/EEC) and with local laws and regulations. All efforts were made to minimize animal suffering and reduce the number of animals used, according to the 3Rs principle. Approval for this study was obtained from the Institutional Ethics Committee on the Use of Animals of the Faculty of Medicine of the University of Coimbra. Prior to surgery, animals were anaesthetized with isoflurane vaporized in O₂ (Vetfluorane, Virbac, Sintra, Portugal). All surgical procedures were done in aseptic conditions. The dorsal regions were disinfected with a povidone-iodine solution (Egrema, Paracélsia, Porto, Portugal) and incisions (length, 1 cm) were made in each quadrant of the dorsal region, at the right/left scapular level and right/left lumbar region, equidistant from the spine. To receive the implants, blunt-tipped scissors were used to bluntly dissect the subcutaneous cellular tissue and create surgical pouches with a mean depth of 20 mm, parallel to the spine. Four root segments (length, 6 mm; internal diameter, 1–1.5 mm) were subcutaneously implanted in each animal. The

incisions were then closed with a 3–0 silk suture (Silkum HR26, B. Braun Surgical, Rubí, Spain). Empty root segments served as a negative control, roots with no biomaterial as experimental control, the roots containing both SCAPs, PRP, and Biomaterial were the experimental groups (Table 2). At the end of the experimental period (4 months) the animals were euthanized, and biopsy samples are collected.

Histology

Biopsies containing the root segments and surrounding tissues (with 1-cm safety margins) were collected and fixed in neutral 10% buffered formaldehyde (Panreac, 143091.1214, Barcelona, Spain). After fixation, tissues were decalcified with Morse’s solution and then sequentially dehydrated in ethanol, cleared in xylol, and impregnated and embedded in Paraplast® (Sigma-Aldrich, P3558, Steinheim, Germany) with the long axis of the root canal parallel to the tissue cassette (Diapath, Martinengo, Italy) basis. Longitudinal serial 5 µm sections were cut, mounted on pre-coated glass slides (Menzel-Glaser, Thermo scientific, Braunschweig, Germany), and stained with hematoxylin and eosin. Two sections from each root segment were selected for analysis and quantification. Image acquisition was performed under brightfield using an Axio Scan.Z1 microscope from Carl Zeiss with a 20x/0.8 Plan-Apochromat lens and digital images acquired and processed using Zen Software (Zeiss). To measure surface areas occupied by different tissues inside the root segment image processing was performed by an observer blind to the treatment and experimental conditions using ImageJ (NIH, Maryland, USA).

Immunocytochemistry

The presence of stem cell markers in SCAPs was assessed, namely, Oct4 (1:400; Abcam ab19857) and SSEA4 (1:66; Abcam ab16287) and the neuronal progenitor marker Nestin (1:500; Millipore ABD69), as well as the early neuronal marker β-III Tubulin (1:200; Millipore MAB1637). Briefly, cells were plated onto µ-Slide 8-well ibiTreat chamber slides

(ibidi), subsequently washed in PBS and fixed with 4% PFA for 20 min at room temperature. Then, cells were washed twice with PBS and permeabilized with 0.2% Triton X-100 in PBS for 2 min and non-specific binding epitopes were blocked by incubating cells with PBS 3% BSA for 30 min. Primary antibodies were incubated in a PBS 3% BSA solution overnight at 4 °C. In the following day, cells were washed twice with PBS and incubated for 2 hours with the secondary antibodies anti-rabbit Alexa Fluor-488 conjugate (Invitrogen A11008) and anti-mouse Alexa Fluor-568 conjugate (Invitrogen A11031), diluted 1:200 in PBS 3% BSA. In some experiments, DNA was stained with Hoechst 33342 (1 µg/mL) for 5 min in the dark, and cells were again washed twice in PBS and kept in PBS at 4 °C until observation. Images were acquired using a Confocal LSM 710 Carl Zeiss microscope, a Plan-Apochromat 40x/1.4 Oil lens, and processed using Zen Software (Zeiss).

Statistical analysis

Data are represented as fractional counts or as mean values ± s.e.m. (as indicated in figure legend). Statistical analysis was performed using two-tailed Fisher’s exact test or one-way ANOVA analysis followed by Holm-Sidak *post hoc* test. Sample normality was tested using D’Agostino-Pearson normality test. Analysis were performed using GraphPad (Prism), and statistical significance was defined as ****P* < 0.001, ***P* < 0.01, **P* < 0.05.

Results

This work started with isolating SCAPs from the apical papilla of third molars with incomplete rhizogenesis. First, a characterization of these cells was performed using immunocytochemistry against pluripotency markers and compared against a culture of human fibroblasts obtained from donor’s gingiva. Using anti-Oct4 and anti-SSEA4 antibodies, a positive signal for both stem cell markers in the dental cell culture was observed, whereas fibroblast did not show a significant signal under the same conditions, suggesting that our culture was rich in SCAPs (Fig. 1a). Similarly, a strong staining against Nestin, an intermediate filament protein that is present in neuroepithelial stem cells and SCAPs, was also observed (Fig. 1b). However, and as expected, SCAPs did not significantly express the mature neuronal marker β-Tubulin III, suggesting the maintenance of a profile closer to that of undifferentiated neuroepithelial progenitor cells. Finally, to assess the multipotency of this population *in vitro*, adipogenesis, chondrogenesis, and osteogenesis differentiation protocols were applied. Successful differentiation into the different cell types was confirmed using Oil Red, Alcian Blue, and Alizarin staining, respectively (Fig. 1c).

Table 2 Grouping of SCAPs implants, PRP, and biomaterials

	SCAPs	PRP	Biomaterial
Group I-ER (empty roots) (<i>n</i> = 11)	-	-	-
Group II-SCAPs (<i>n</i> = 21)	+	+	-
Group III-MTA (<i>n</i> = 11)	+	+	MTA
Group IV-BD (<i>n</i> = 10)	+	+	Biodentine

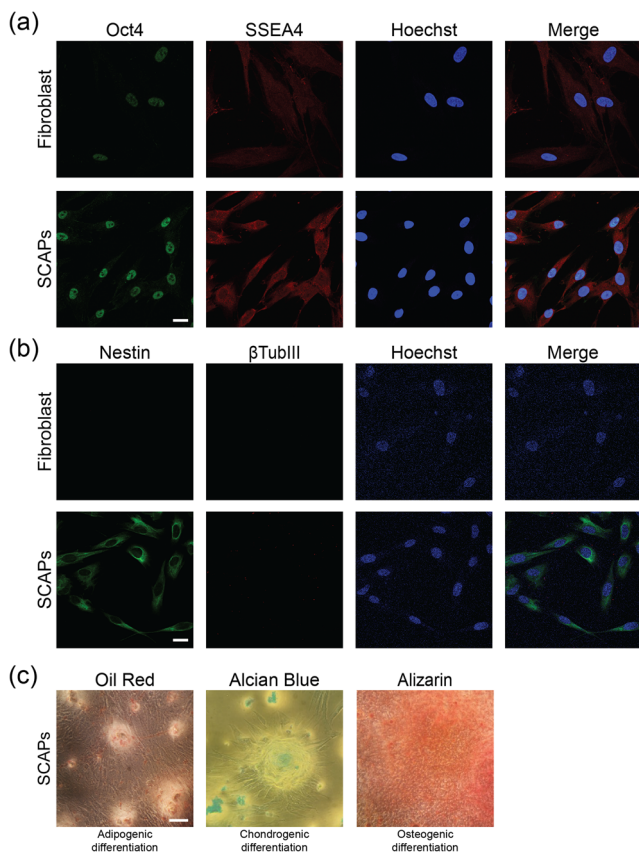


Fig. 1 Differentiation potential and stem cell marker expression in SCAPs. **a** Labelling for Oct4 and SSEA4 was performed under the same conditions for SCAPs and human skin fibroblasts, and Hoechst used to visualise nuclei. Significant labelling for both markers was seen in SCAPs but not in fibroblasts. **b** SCAPs stain positively for Nestin, a neuronal precursor marker but similarly to fibroblast, were negative for β -Tubulin III, a marker of mature neurons. Scale bar = 20 μ m. **c** The differentiation potential of the SCAPs culture was observed following adipogenesis, chondrogenesis and osteogenesis differentiation, positive response was evaluated by staining with Oil Red, Alcian Blue, and Alizarin. Scale bar = 100 μ m

To further characterize SCAP cultures following *in vitro* expansion, samples collected from four individuals were selected, and flow cytometry analysis was performed using a combination of surface markers. The obtained results showed a cell population strongly positive for CD44, CD73, CD105 and CD146, also expressing STRO-1 and CD24 (Figs. 2a–g). This population was negative for CD14 and CD45 (Figs. 2h–i). As a negative control, CD14 and CD45 hematopoietic stem cell markers were selected since they are widely used as negative markers for mesenchymal and dental stem cell populations.

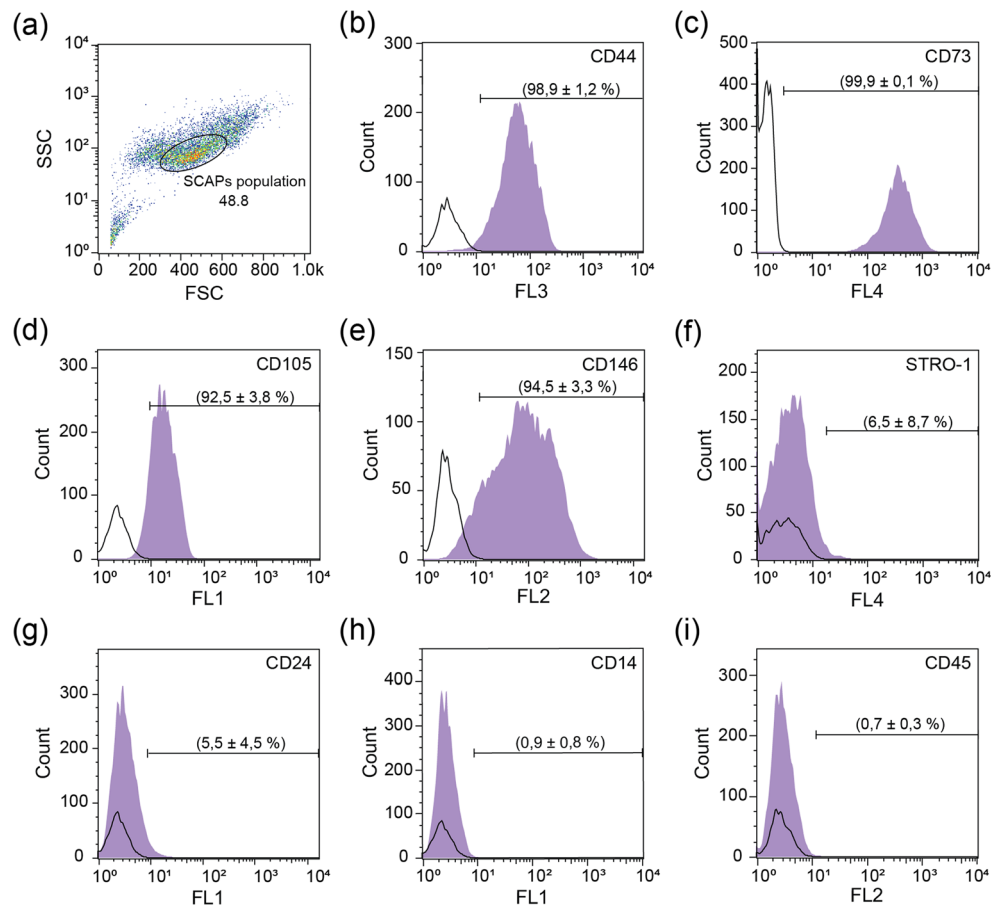
To assess the potential of these cells to regenerate dentine and pulp formation when applied together with a bioactive material, we prepared dental root segments that were filled with mixture of SCAPs and PRP, a biological scaffold. Treated and disinfected roots were randomly assigned to one of four groups, as summarized in Table 2. Four roots were

subcutaneously implanted in the dorsal region of immunodeficient RNU nude rats for a period of 4 months. At the end of this period, during sample collection, blood vessels in close apposition or penetrating the open apex of the canals were observed in groups II–IV (Fig. 3a). Histological characterization of all implants was performed using hematoxylin and eosin (H&E) staining.

In group I-ER, which contained only empty roots, a fibrous capsule surrounding the root construct was observed, separating the root fragment from the subcutaneous tissues of the dermal space of the rat. Approximately a third (32%) of all sections analyzed for this group were found empty, with no tissue present in the lumen of the canal (Fig. 3b). The remainder two thirds (68%) showed an infiltration of soft connective tissue (Fig. 3c).

In sections collected from implants from Group II-SCAPs, containing SCAPs embedded in a PRP matrix, 15% of root segments were empty, while 85% of sections showed the formation of a well-organized complex tissue (Fig. 3d). These were associated with neural innervation and infiltration of a blood network (Figs. 3e–f). The presence of *de novo* deposited tissue, resembling pulp and dentin-like structures, was observed in 27% of sections in this group (Figs. 3g–i). Cells and debris were found embedded in the matrix of this new tissue inside of the root canal lumen. Dentin-like tissue appeared in continuum with original canal dentin walls of the root segment (Figs. 3h, white arrowhead). The new mineralized tissue did not present a uniform thickness and it was possible to observe two layers: a darker “hard” tissue, and a more recently deposited layer, eosinophilic, resembling predentin. Higher magnification analysis allowed the identification of cells with ramified projections, similar to canaliculi of putative cementocytes (Figure 3h, arrow); as well as a clear layer of odontoblast-like cells aligned against the pulp side of the newly formed dentin-like tissue (Figure 3h-i, arrowhead). In some samples, the presence of organized, parallel “pre-dentinal” tubules, containing projection from the odontoblast-like cells, could be seen (Fig. 3i, star). Distally to these, the presence of mineralized globular dentine was also detected (Fig. 3i, arrow). Moreover, the “soft” tissue present in these root segments, even when no dentin was deposited, was similar to a pulp-like structure, unlike the soft connective tissue present in sections from Group I. However, to avoid ambiguity, all non-dentin-like tissue in groups II–IV, was still classified as “soft,” since the explanted cells could not reliably be distinguished, under H&E staining, from invading rat cells. Nevertheless, to ascertain if the regenerated tissue was of human origin, immunohistochemistry was performed using an antibody that detects a protein component of mitochondria that is exclusively found in the human organelle. Qualitative analysis revealed that cells originating pulp-like tissue in the lumen of the root segments were indeed of human origin (Fig. 3j).

Fig. 2 Surface marker analysis in SCAPs isolated from four individual donors. **a–i** Gating strategy was selected to exclude debris using a forward scatter area (FSC) versus side scatter area (SSC) gate followed by a selection of dead/live cells using 7-amino-actinomycin D labelling ($n = 4$). **b–e** The common mesenchymal stem cell markers, CD44, CD73, CD105, and CD146 strongly (> 90%) labelled the population of SCAPs from each donor individual (average results presented as a percentage of total cells). **f–g** STRO-1 and CD24 label a subpopulation of SCAPs, showing an average rate of positive cells of 6.5 and 5.5%, respectively. **h–i** The negative control markers CD14 and CD45, characteristic of hematopoietic stem cells, show negligibly frequency count (< 1%) in SCAPs cultures. The open area curve represents the unstained cells, and the shaded area represents the specific marker



Roots from Group III-MTA contained SCAPs, PRP and a ProRoot MTA barrier. A fraction (28%) of ProRoot MTA samples showed new hard tissue formation (Figs. 4a–b) with similar characteristics to those present in Group II-SCAPs. In some instances, it was possible to observe the formation of a dentinal bridge (Fig. 4b, arrow) apposed to the ProRoot MTA barrier (Fig. 4b, star). Similarly, Group IV-BD consisted of root implants with SCAPs, PRP and a Biodentine barrier. In Biodentine samples, 20% of sample also presented regenerated hard tissues, and we could also identify the formation of dentinal bridges on the inner surface of the cement (Fig. 4c, star). Similarly, cellular projections were found inside the root segment original dentinal tubules (Fig. 4d, arrow), and odontoblast-like cells (Figs. 4d–e, arrowhead) could be found projecting into de novo formed dentin (Figure 4e). Qualitatively, no significant differences were found between Groups II-SCAPs, III-MTA and IV-BD, regarding the morphology of the tissues formed or the diversity of cellular elements encountered.

A quantitative analysis of the obtained results found that the presence of mineralized tissue was significantly linked to the insertion of SCAPs + PRP within the empty roots (Two-sided Fisher’s exact test; $P = 0.005$; Empty roots = 0/11; Roots with SCAPs = 11/30; Hard tissue/No Hard tissue present)

(Figure 5a). It was also noted that the presence of biomaterials (ProRoot MTA or Biodentine) could influence the viability of the designed preparation, as there was significant difference in the fraction of implants that formed *de novo* tissue (Two-sided Fisher’s exact test; $P = 0.0061$, No biomaterial = 35/6 x MTA group = 11/11; and $P = 0.0238$, No biomaterial = 35/6 x Biodentine group = 11/9; Tissue formed/No tissue formed) (Figure 5b–c). However, there were no differences in the fraction of roots with tissue formed when comparing between both biomaterials (Two-sided Fisher’s exact test; $P = 0.7675$), nor in the fraction of roots with presence of hard tissue (Two-sided Fisher’s exact test; $P > 0.5$) (Figure 5b–c).

The area occupied by soft tissue was measured, including infiltrated connective tissue or any other that did not contain mineralized hard deposits, and showed no statistical difference between groups (One-Way ANOVA $F_{(3, 70)} = 2,616$; $P > 0.05$) (Fig. 5d). Regarding the percentage of the internal root implant filled with hard material, ProRoot MTA showed a smaller percentage of total area covered by mineralized tissue, while the Biodentine group showed a significant increase in total area covered (One-Way ANOVA $F_{(3, 32)} = 76,74 = 2,616$; $P < 0.001$; post-hoc analysis: Holm-Sidak $G_{(II \times III)} P < 0.01$; $G_{(II \times IV)} P < 0.001$; $G_{(III \times IV)} P < 0.001$) (Fig. 5d).

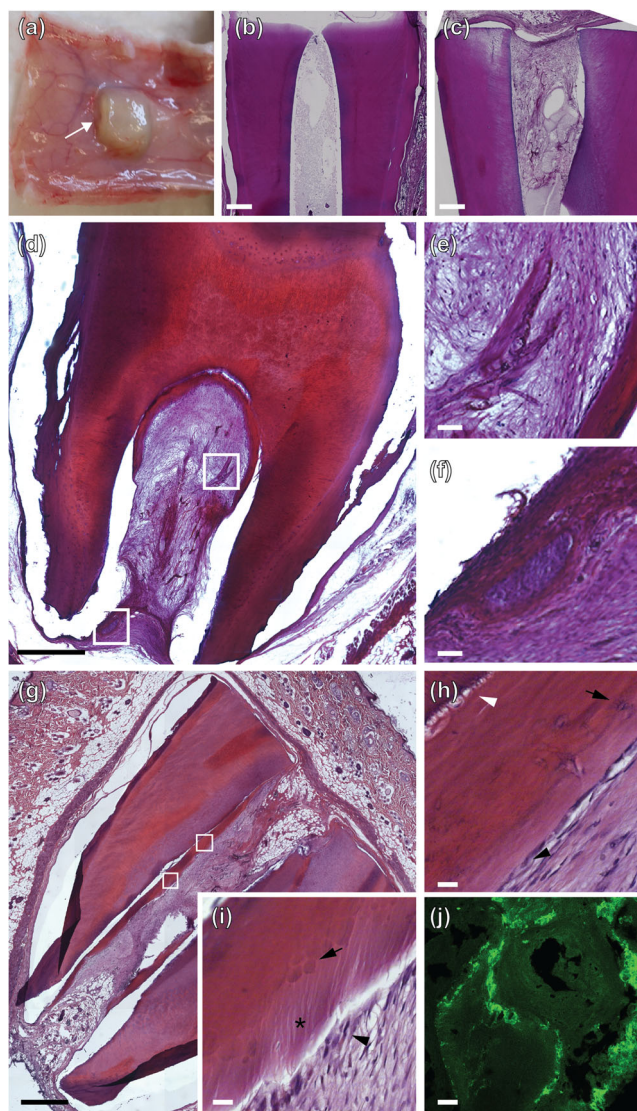


Fig. 3 SCAPs in implanted root canal segments give rise to novel dentin deposition. **a** Implanted root segments were dissected out after a 4-month experimental period, often exhibiting vasculature infiltrating the root apex. **b–c** Root segments from Group I-ER, presented either an empty canal (**b**) or the presence of loose connective tissue (**c**), presumably due to infiltration of rat cells. **d–i** Root segments from Group II-SCAPs, gave rise to pulp-like and dentin-like tissue that was formed *de novo* (**d**). Microscopically, blood vessel (**e**) and neural innervation (**f**) could be seen in proximity to the new tissue formed in the canal. Dentin-like tissue was found apposed to the original dentin in the implanted root (**h**, white arrowhead). Odontoblast-like cells were found aligned against the pulp side of the dentin-like tissue (**h–i**, dark arrowhead), and cementocyte-like cells were also present embedded in the dentine matrix (**h**, arrow). Pre-dentinal tubules (**i**, star) and mineralized dentine globules (**i**, arrow) could also be observed. (**j**) Staining with an anti-human mitochondria antibody reveals significant positive staining inside the root canal. Scale bars: 500 μm in **b–d**, **g**; 50 μm **e–f** and 20 μm in **h–j**

Discussion

This study assessed the potential of using SCAPs in a PRP scaffold for regenerative endodontic procedures, in association with ProRoot MTA or Biodentine. Regenerative

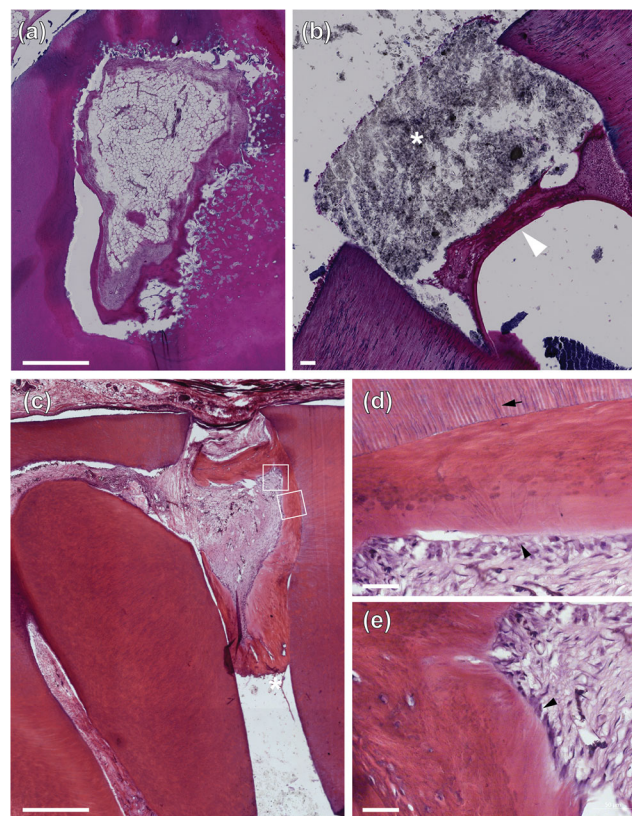


Fig. 4 SCAPs in contact with ProRoot MTA and Biodentine give rise to novel dentin deposition and dentin bridges. **a** Transversal cut of root segment reveals a continuous ring of dentin deposition. **b–c** In apposition to the ProRoot MTA (**b**) and Biodentine (**c**) barrier a dentinal bridge could be observed (star). **d–e** Presence of cellular diversity, morphology of dentin deposition, presence of odontoblast-like cells (arrowhead), and cellular projections into pre-existing dentin tubules (arrow) were observed in conditions containing either biomaterials. Scale bar 500 μm in **a,c** and 50 μm in **b, d–e**

endodontics is defined by the American Association of Endodontics Glossary of Endodontic Terms as “biologically-based procedures designed to physiologically replace damaged tooth structures, including dentin and root structures, as well as cells from the pulp-dentin complex.” The present work provides evidence of *de novo* formation of pulp and dentin-like tissues in the empty canal space of root segments filled with cells cultured from isolated apical papilla and implanted in the subcutaneous space of immunodeficient rats. This *in vivo* model mimics a clinical setting where the regeneration of a permanent tooth with necrosis may be rescued. This model also combines several relevant aspects: (i) experimental constructs are made from human root segments, which best replicate the clinical setting; (ii) root segments provide a potential reservoir for dentin-derived growth factors which may be mobilized after treatment with EDTA [41]; (iii) SCAPs were chosen in this study since they are not as well studied as other DSCs niches, but may play a crucial role during dentin-pulp complex regeneration [42]; (iv) PRP was used as a simple and effective scaffold that may be readily prepared

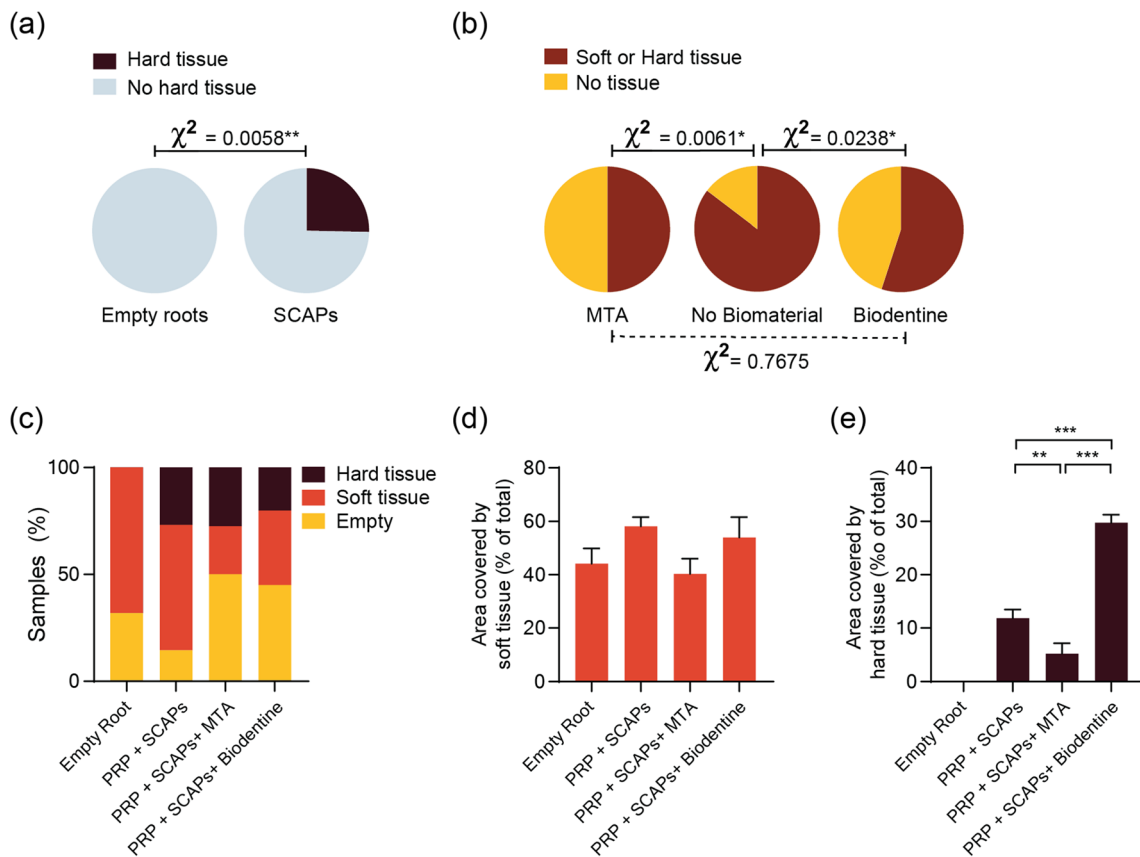


Fig. 5 Quantification of hard tissue deposition and surface area deposited in histological sections from implants. **a** Fraction of sections with root segments containing novel dentin deposition was restricted to the groups containing SCAPs (Two-sided Fisher’s exact test). **b** The presence of biomaterial influences the fraction of roots containing no tissue present, however, there was no statistically significant difference when comparing between ProRoot MTA and Biodentine groups (Two-sided Fisher’s exact test), $n = 20–41$. **c** Histogram distribution of fractional section count of

sections containing no visible cells (Empty), soft tissue (loose connective or pulp-like) or hard tissue (dentin-like tissue). **d–e** Quantification of canal interior area covered by soft (d) or hard tissue (e) in section from all four experimental groups; One-Way ANOVA with Holm-Sidak *post hoc* test; $n = 11–35$ for d and $n = 4–15$ for e. Data are presented as fractional counts or means \pm s.e.m. Statistical significance: * $P < 0.05$, ** $P < 0.01$, *** $P < 0.001$

from each individual; and (v) the potential application of two bioactive materials with relevance in the clinical setting was also assessed.

Root canal dentin acts as an endogenous source of bioactive molecules that may become exposed to stimulate chemotaxis, cellular proliferation, differentiation and angiogenesis [43]. A plethora of dentin matrix molecules and growth factors may be exposed on root dentinal surface by chemical treatment with EDTA. This has been shown to promote dental pulp stem cell adhesion, migration, and differentiation [41]. Other studies have shown evidence that EDTA irrigation supports survival of SCAPs [44] and the attachment of dental pulp stem cells [45]. Additionally, it has also been demonstrated that bioactive cements may further facilitate the solubilization of dentine matrix molecules, such as TGF- β 1, NGF and GDNF, and stimulate tertiary dentinogenesis [46]. However, by themselves, dentinal matrix substances fail to originate any dentin-like tissue or any pulp-like tissue when there were no SCAPs introduced in root segments. The soft tissue observed

in the “empty” roots was largely loose connective tissue that invaded the canal interior, most likely via cell homing effects promoted by dentinal-released growth factors. Conversely, the soft tissue in groups containing SCAPs (II–IV) was mostly pulp-like upon histological analysis, even when no dentin-like “hard” material was present. In this study, for unambiguous quantification, we decided to focus our analysis mostly on the material clearly presenting dentin-like morphology and structure.

In general, DSCs provide an attractive population to be used in clinical applications, since biobanking may be possible at different timepoints, e.g., from the pulp of deciduous teeth in young children or later and from third molars (pulp or SCAPs) in young adults. Additionally, DSCs have been proposed to be amenable to cryopreservation as they may retain pluripotency and regenerative properties even after cell freezing [47]. In line with this, the present work also supports this conclusion, since all the explanted cells were originated from a frozen stock. In fact, DSCs have now been used in human

trials to restore pulp vitality [24, 25]; however, the potential for using SCAPs in clinical procedures has not yet been widely explored [48].

In order to conveniently apply DSCs, several scaffolds have been tested for pulp-dentin tissue engineering [49, 50]. The ideal scaffold should be biocompatible and biodegradable and release growth factors. In this study PRP was used, since it is a natural scaffold that presents good results in supporting pulp-like tissue formation *in vivo* [51]. PRP was obtained from a donor's venous blood via differential centrifugation, and coagulation was then triggered by adding CaCl_2 , which resulted in a 3-dimensional fibrin-based network containing captive platelets, cytokines and growth factors, such as TGF- β , platelet derived-growth factor, vascular endothelial growth factor, insulin like growth factor and fibroblast growth factor [52, 53].

After being cultured *in vitro*, apical papilla cells were found to remain largely homogeneous regarding the expression of stem cell markers (Oct4 and SSEA4) and the expression of typical MSC surface markers (e.g., CD44, CD73, CD105, or CD146). While it was expected that some fibroblasts were also present in this culture, the obtained cells were positive for Oct4 and Nestin, while fibroblasts were not, again suggesting a population strongly enriched in SCAPs. However, even if fibroblasts contaminate these culture preparations, recent studies have shown that fibroblasts produce significant amounts of biologically active molecules [54, 55], which may then act on stem cell recruitment and differentiation [56, 57], neo-angiogenesis [58, 59], or neural growth [60].

Histological observation revealed that approximately 70% of samples of “empty” roots presented infiltration of loose connective tissue, which was likely due to infiltration of host cells. Nevertheless, *de novo* deposition of dentin (i.e., hard tissue) and pulp-like tissue formation was only observed when SCAPs and PRP were applied. The deposition of a layer of dentin-like structure was always seen in apposition to dentinal walls or the surface of the biomaterial, and *de novo* dentin was never found within the pulp-like strata. This may be due to the biophysical properties of existing dentin interacting with SCAP-derived odontoblasts or to the higher concentration of bioactive molecules on the root dentin wall.

In addition to the presence of pulp-like tissue, blood vessels and nerve fibres, a typical layer of odontoblast-like cells in the pulp side of the new novel dentin tissue could also be observed. These odontoblast-like cells adopted a histological and cytological organization, with columnar shape and cellular polarization and cytoplasmic processes extending into dentinal tubules, similar to what is found in odontoblasts *in vivo* [61]. Additionally, the presence of cementocyte-like cells, presenting distinctive ramifications [61], further highlights the variety of cells present in the explants. Regarding the presence of empty root canals in all experimental groups, we can attribute these to the mechanical difficulty in precisely inserting the cellular suspension due to the time-sensitive coagulation

of PRP and a relatively low concentration of cells per root segment ($>1 \times 10^6$ cells/mL). While another possibility could be loss of the explanted cells due to infection, only one implant was lost due to such an event.

Regarding the two biomaterials, no differences were found in the frequency to which they generated samples with significant amount of hard tissue. However, the area covered by novel dentin was significantly greater for Biodentine. We previously found that Biodentine eluates produce changes in cellular metabolic activity and cellular replication during wound healing assay [33], showing that high concentrations of Biodentine in cell culture media significantly decrease stem cell proliferation [62, 63]. However, as we previously hypothesized [33], one possibility is that Biodentine may enhance the differentiation of stem cells. This has been shown to be the case as Biodentine induces formation of odontoblasts and promotes mineralization [64]. Moreover, it also possesses immunomodulatory properties beneficial for tissue healing as it has been shown to suppress pro-inflammatory and augment anti-inflammatory cytokine expression [65]. The data presented here further supports this hypothesis and provides *in vivo* evidence that supports a role for this biomaterial in enhancing deposition of dentin.

Finally, we also note the lack of formation of teratomas or other abnormal masses in the present work. This speaks to the relative safety in applying SCAPs in the context of a micro-environment that closely mimics their natural niche.

Conclusion

The present study allowed to conclude that ProRoot MTA and Biodentine, when used with SCAPs isolated from molars with incomplete rhizogenesis, displayed good biocompatibility and promoted the formation of pulp-dentin complex and dentinal bridges. However, ProRoot MTA displayed a small but significant lower area of hard tissue formed when compared with the control condition, while Biodentine performed significantly better in this metric, which allowed us to reject our null hypothesis. Together, these results highlight the importance of combining *in vitro* studies with *in vivo* experiments that may offer closer approximation to clinically relevant settings when assessing potential advantages between different biomaterials. This is particularly relevant in the study of material and procedural variables, due to the increased efforts to apply dental stem cells in clinical application.

Acknowledgments The authors thank Cláudia Brites, dedicated technician of the Hard Tissues Histology Laboratory, Faculty of Medicine, University of Coimbra, for assisting with the histological processing and staining. This project received funding from GAI, Gabinete Apoio à Investigação, Faculty of Medicine, University of Coimbra and the European Union's Horizon 2020 research and innovation programme

under grant agreement Number 799164. This work was financed by the European Regional Development Fund (ERDF), through the Centro 2020 and through the COMPETE 2020 - Operational Programme for Competitiveness and Internationalisation and Portuguese national funds via FCT – Fundação para a Ciência e a Tecnologia, under project UIDB/04539/2020.

Declarations

Ethical approval The procedures and study protocol described here were approved by the Ethics Committee of the Faculty of Medicine, University of Coimbra (Project CE-028/2016) and following the guidelines of the Declaration of Helsinki.

Informed consent Informed consent was obtained from all individual participants included in the study.

Conflict of interest The authors declare no conflict of interest.

References

- Till JE, Mc CE (1961) A direct measurement of the radiation sensitivity of normal mouse bone marrow cells. *Radiat Res* 14:213–222
- Li L, Xie T (2005) Stem cell niche: structure and function. *Annu Rev Cell Dev Biol* 21:605–631. <https://doi.org/10.1146/annurev.cellbio.21.012704.131525>
- Morrison SJ, Spradling AC (2008) Stem cells and niches: mechanisms that promote stem cell maintenance throughout life. *Cell* 132:598–611. <https://doi.org/10.1016/j.cell.2008.01.038>
- Gronthos S, Mankani M, Brahimi J, Robey PG, Shi S (2000) Postnatal human dental pulp stem cells (DPSCs) in vitro and in vivo. *Proc Natl Acad Sci U S A* 97:13625–13630. <https://doi.org/10.1073/pnas.240309797>
- Miura M, Gronthos S, Zhao M, Lu B, Fisher LW, Robey PG, Shi S (2003) SHED: stem cells from human exfoliated deciduous teeth. *Proc Natl Acad Sci U S A* 100:5807–5812. <https://doi.org/10.1073/pnas.0937635100>
- Seo BM, Miura M, Gronthos S, Bartold PM, Batouli S, Brahimi J, Young M, Robey PG, Wang CY, Shi S (2004) Investigation of multipotent postnatal stem cells from human periodontal ligament. *Lancet* 364:149–155. [https://doi.org/10.1016/S0140-6736\(04\)16627-0](https://doi.org/10.1016/S0140-6736(04)16627-0)
- Morszeck C, Gotz W, Schierholz J, Zeilhofer F, Kuhn U, Mohl C, Sippel C, Hoffmann KH (2005) Isolation of precursor cells (PCs) from human dental follicle of wisdom teeth. *Matrix Biol* 24:155–165. <https://doi.org/10.1016/j.matbio.2004.12.004>
- Sonoyama W, Liu Y, Fang D, Yamaza T, Seo BM, Zhang C, Liu H, Gronthos S, Wang CY, Wang S et al (2006) Mesenchymal stem cell-mediated functional tooth regeneration in swine. *PLoS One* 1:e79. <https://doi.org/10.1371/journal.pone.0000079>
- Sonoyama W, Liu Y, Yamaza T, Tuan RS, Wang S, Shi S, Huang GT (2008) Characterization of the apical papilla and its residing stem cells from human immature permanent teeth: a pilot study. *J Endod* 34:166–171. <https://doi.org/10.1016/j.joen.2007.11.021>
- Volponi AA, Pang Y, Sharpe PT (2010) Stem cell-based biological tooth repair and regeneration. *Trends Cell Biol* 20:715–722. <https://doi.org/10.1016/j.tcb.2010.09.012>
- Zhang W, Walboomers XF, Shi S, Fan M, Jansen JA (2006) Multilineage differentiation potential of stem cells derived from human dental pulp after cryopreservation. *Tissue Eng* 12:2813–2823. <https://doi.org/10.1089/ten.2006.12.2813>
- Kim BC, Bae H, Kwon IK, Lee EJ, Park JH, Khademhosseini A, Hwang YS (2012) Osteoblastic/cementoblastic and neural differentiation of dental stem cells and their applications to tissue engineering and regenerative medicine. *Tissue Eng Part B Rev* 18:235–244. <https://doi.org/10.1089/ten.TEB.2011.0642>
- Nuti N, Corallo C, Chan BM, Ferrari M, Gerami-Naini B (2016) Multipotent differentiation of human dental pulp stem cells: a literature review. *Stem Cell Rev Rep* 12:511–523. <https://doi.org/10.1007/s12015-016-9661-9>
- Chalisserry EP, Nam SY, Park SH, Anil S (2017) Therapeutic potential of dental stem cells. *J Tissue Eng* 8:2041731417702531. <https://doi.org/10.1177/2041731417702531>
- Mita T, Furukawa-Hibi Y, Takeuchi H, Hattori H, Yamada K, Hibi H, Ueda M, Yamamoto A (2015) Conditioned medium from the stem cells of human dental pulp improves cognitive function in a mouse model of Alzheimer's disease. *Behav Brain Res* 293:189–197. <https://doi.org/10.1016/j.bbr.2015.07.043>
- Yang KL, Chen MF, Liao CH, Pang CY, Lin PY (2009) A simple and efficient method for generating Nurr1-positive neuronal stem cells from human wisdom teeth (tNSC) and the potential of tNSC for stroke therapy. *Cytotherapy* 11:606–617. <https://doi.org/10.1080/14653240902806994>
- Gandia C, Arminan A, Garcia-Verdugo JM, Lledo E, Ruiz A, Minana MD, Sanchez-Torrijos J, Paya R, Mirabet V, Carbonell-Uberos F et al (2008) Human dental pulp stem cells improve left ventricular function, induce angiogenesis, and reduce infarct size in rats with acute myocardial infarction. *Stem Cells* 26:638–645. <https://doi.org/10.1634/stemcells.2007-0484>
- Ishikawa J, Takahashi N, Matsumoto T, Yoshioka Y, Yamamoto N, Nishikawa M, Hibi H, Ishiguro N, Ueda M, Furukawa K et al (2016) Factors secreted from dental pulp stem cells show multifaceted benefits for treating experimental rheumatoid arthritis. *Bone* 83:210–219. <https://doi.org/10.1016/j.bone.2015.11.012>
- Chen YJ, Zhao YH, Zhao YJ, Liu NX, Lv X, Li Q, Chen FM, Zhang M (2015) Potential dental pulp revascularization and odonto-osteogenic capacity of a novel transplant combined with dental pulp stem cells and platelet-rich fibrin. *Cell Tissue Res* 361:439–455. <https://doi.org/10.1007/s00441-015-2125-8>
- Hayashi Y, Murakami M, Kawamura R, Ishizaka R, Fukuta O, Nakashima M (2015) CXCL14 and MCP1 are potent trophic factors associated with cell migration and angiogenesis leading to higher regenerative potential of dental pulp side population cells. *Stem Cell Res Ther* 6:111. <https://doi.org/10.1186/s13287-015-0088-z>
- Gronthos S, Brahimi J, Li W, Fisher LW, Cherman N, Boyde A, DenBesten P, Robey PG, Shi S (2002) Stem cell properties of human dental pulp stem cells. *J Dent Res* 81:531–535. <https://doi.org/10.1177/154405910208100806>
- Cordeiro MM, Dong Z, Kaneko T, Zhang Z, Miyazawa M, Shi S, Smith AJ, Nor JE (2008) Dental pulp tissue engineering with stem cells from exfoliated deciduous teeth. *J Endod* 34:962–969. <https://doi.org/10.1016/j.joen.2008.04.009>
- Rosa V, Zhang Z, Grande RH, Nor JE (2013) Dental pulp tissue engineering in full-length human root canals. *J Dent Res* 92:970–975. <https://doi.org/10.1177/0022034513505772>
- Nakashima M, Iohara K, Murakami M, Nakamura H, Sato Y, Arijii Y, Matsushita K (2017) Pulp regeneration by transplantation of dental pulp stem cells in pulpitis: a pilot clinical study. *Stem Cell Res Ther* 8:61. <https://doi.org/10.1186/s13287-017-0506-5>
- Xuan K, Li B, Guo H, Sun W, Kou X, He X, Zhang Y, Sun J, Liu A, Liao L et al (2018) Deciduous autologous tooth stem cells regenerate dental pulp after implantation into injured teeth. *Sci Transl Med* 10. <https://doi.org/10.1126/scitranslmed.aaf3227>
- Na S, Zhang H, Huang F, Wang W, Ding Y, Li D, Jin Y (2016) Regeneration of dental pulp/dentine complex with a three-dimensional and scaffold-free stem-cell sheet-derived pellet. *J*

- Tissue Eng Regen Med 10:261–270. <https://doi.org/10.1002/term.1686>
27. Palma PJ, Ramos JC, Martins JB, Diogenes A, Figueiredo MH, Ferreira P, Viegas C, Santos JM (2017) Histologic evaluation of regenerative endodontic procedures with the use of chitosan scaffolds in immature dog teeth with apical periodontitis. *J Endod* 43:1279–1287. <https://doi.org/10.1016/j.joen.2017.03.005>
 28. Chen X, Bao ZF, Liu Y, Liu M, Jin XQ, Xu XB (2013) Regenerative endodontic treatment of an immature permanent tooth at an early stage of root development: a case report. *J Endod* 39:719–722. <https://doi.org/10.1016/j.joen.2012.12.023>
 29. Xu J, Gou L, Zhang P, Li H, Qiu S (2020) Platelet-rich plasma and regenerative dentistry. *Aust Dent J* 65:131–142. <https://doi.org/10.1111/adj.12754>
 30. Meschi N, Castro AB, Vandamme K, Quiryren M, Lambrechts P (2016) The impact of autologous platelet concentrates on endodontic healing: a systematic review. *Platelets* 27:613–633. <https://doi.org/10.1080/09537104.2016.1226497>
 31. Alsousou J, Ali A, Willett K, Harrison P (2013) The role of platelet-rich plasma in tissue regeneration. *Platelets* 24:173–182. <https://doi.org/10.3109/09537104.2012.684730>
 32. Gong T, Heng BC, Lo EC, Zhang C (2016) Current advance and future prospects of tissue engineering approach to dentin/pulp regenerative therapy. *Stem Cells Int* 2016:9204574. <https://doi.org/10.1155/2016/9204574>
 33. Sequeira DB, Seabra CM, Palma PJ, Cardoso AL, Peça J, Santos JM (2018) Effects of a New Bioceramic Material on Human Apical Papilla Cells. *J Funct Biomater* 9:74. <https://doi.org/10.3390/jfb9040074>
 34. Saberi EA, Karkehabadi H, Mollashahi NF (2016) Cytotoxicity of various endodontic materials on stem cells of human apical papilla. *Iran Endod J* 11:17–22. <https://doi.org/10.7508/iej.2016.01.004>
 35. Araujo LB, Cosme-Silva L, Fernandes AP, Oliveira TM, Cavalcanti BDN, Gomes Filho JE, Sakai VT (2018) Effects of mineral trioxide aggregate, Biodentine™ and calcium hydroxide on viability, proliferation, migration and differentiation of stem cells from human exfoliated deciduous teeth. *J Appl Oral Sci* 26:e20160629. <https://doi.org/10.1590/1678-7757-2016-0629>
 36. Paranjpe A, Zhang H, Johnson JD (2010) Effects of mineral trioxide aggregate on human dental pulp cells after pulp-capping procedures. *J Endod* 36:1042–1047. <https://doi.org/10.1016/j.joen.2010.02.013>
 37. D'Anto V, Di Caprio MP, Ametrano G, Simeone M, Rengo S, Spagnuolo G (2010) Effect of mineral trioxide aggregate on mesenchymal stem cells. *J Endod* 36:1839–1843. <https://doi.org/10.1016/j.joen.2010.08.010>
 38. Pelepenko LE, Saavedra F, Antunes TBM, Bombarda GF, Gomes B, Zaia AA, Camilleri J, Marciano MA (2021) Physicochemical, antimicrobial, and biological properties of White-MTAFlow. *Clin Oral Investig* 25:663–672. <https://doi.org/10.1007/s00784-020-03543-7>
 39. Palma PJ, Marques JA, Falacho RI, Correia E, Vinagre A, Santos JM, Ramos JC (2019) Six-Month Color Stability Assessment of Two Calcium Silicate-Based Cements Used in Regenerative Endodontic Procedures. *J Funct Biomater* 10. <https://doi.org/10.3390/jfb10010014>
 40. Sequeira D, Palma P, Diogo P, Cardoso A, Santos JM (2016) The effect of calcium silicate-based cements on viability of stem cells within apical papilla. *Int Endod J* 0:1–90
 41. Galler KM, Widbiller M, Buchalla W, Eidt A, Hiller KA, Hoffer PC, Schmalz G (2016) EDTA conditioning of dentine promotes adhesion, migration and differentiation of dental pulp stem cells. *Int Endod J* 49:581–590. <https://doi.org/10.1111/iej.12492>
 42. Huang GT, Sonoyama W, Liu Y, Liu H, Wang S, Shi S (2008) The hidden treasure in apical papilla: the potential role in pulp/dentin regeneration and bioroot engineering. *J Endod* 34:645–651. <https://doi.org/10.1016/j.joen.2008.03.001>
 43. Smith AJ, Scheven BA, Takahashi Y, Ferracane JL, Shelton RM, Cooper PR (2012) Dentine as a bioactive extracellular matrix. *Arch Oral Biol* 57:109–121. <https://doi.org/10.1016/j.archoralbio.2011.07.008>
 44. Trevino EG, Patwardhan AN, Henry MA, Perry G, Dybdal-Hargreaves N, Hargreaves KM, Diogenes A (2011) Effect of irrigants on the survival of human stem cells of the apical papilla in a platelet-rich plasma scaffold in human root tips. *J Endod* 37:1109–1115. <https://doi.org/10.1016/j.joen.2011.05.013>
 45. Ring KC, Murray PE, Namerow KN, Kuttler S, Garcia-Godoy F (2008) The comparison of the effect of endodontic irrigation on cell adherence to root canal dentin. *J Endod* 34:1474–1479. <https://doi.org/10.1016/j.joen.2008.09.001>
 46. da Rosa WLO, Piva E, da Silva AF (2018) Disclosing the physiology of pulp tissue for vital pulp therapy. *Int Endod J* 51:829–846. <https://doi.org/10.1111/iej.12906>
 47. Hilkens P, Driesen RB, Wolfs E, Gervois P, Vanganswinkel T, Ratajczak J, Dillen Y, Bronckaers A, Lambrechts I (2016) Cryopreservation and Banking of Dental Stem Cells. *Adv Exp Med Biol* 951:199–235. https://doi.org/10.1007/978-3-319-45457-3_17
 48. Palma PJ, Martins J, Diogo P, Sequeira D, Ramos JC, Diogenes A, Santos JM (2019) Does apical papilla survive and develop in apical periodontitis presence after regenerative endodontic procedures? *Appl Sci* 9:3942
 49. Jazayeri HE, Lee SM, Kuhn L, Fahimipour F, Tahiri M, Tayebi L (2020) Polymeric scaffolds for dental pulp tissue engineering: A review. *Dent Mater* 36:e47–e58. <https://doi.org/10.1016/j.dental.2019.11.005>
 50. Galler KM, D'Souza RN, Hartgerink JD, Schmalz G (2011) Scaffolds for dental pulp tissue engineering. *Adv Dent Res* 23:333–339. <https://doi.org/10.1177/0022034511405326>
 51. Galler KM, Brandl FP, Kirchhof S, Widbiller M, Eidt A, Buchalla W, Gopferich A, Schmalz G (2018) Suitability of different natural and synthetic biomaterials for dental pulp tissue engineering. *Tissue Eng A* 24:234–244. <https://doi.org/10.1089/ten.TEA.2016.0555>
 52. Blair P, Flaumenhaft R (2009) Platelet alpha-granules: basic biology and clinical correlates. *Blood Rev* 23:177–189. <https://doi.org/10.1016/j.blre.2009.04.001>
 53. Anitua E, Alkhraisat MH, Orive G (2012) Perspectives and challenges in regenerative medicine using plasma rich in growth factors. *J Control Release* 157:29–38. <https://doi.org/10.1016/j.jconrel.2011.07.004>
 54. Jeanneau C, Lundy FT, El Karim IA, About I (2017) Potential therapeutic strategy of targeting pulp fibroblasts in dentin-pulp regeneration. *J Endod* 43:S17–S24. <https://doi.org/10.1016/j.joen.2017.06.007>
 55. Chmilewsky F, Jeanneau C, Laurent P, About I (2014) Pulp fibroblasts synthesize functional complement proteins involved in initiating dentin-pulp regeneration. *Am J Pathol* 184:1991–2000. <https://doi.org/10.1016/j.ajpath.2014.04.003>
 56. Mathieu S, Jeanneau C, Sheibat-Othman N, Kalaji N, Fessi H, About I (2013) Usefulness of controlled release of growth factors in investigating the early events of dentin-pulp regeneration. *J Endod* 39:228–235. <https://doi.org/10.1016/j.joen.2012.11.007>
 57. Chmilewsky F, Jeanneau C, Laurent P, Kirschfink M, About I (2013) Pulp progenitor cell recruitment is selectively guided by a C5a gradient. *J Dent Res* 92:532–539. <https://doi.org/10.1177/0022034513487377>
 58. Tran-Hung L, Laurent P, Camps J, About I (2008) Quantification of angiogenic growth factors released by human dental cells after injury. *Arch Oral Biol* 53:9–13. <https://doi.org/10.1016/j.archoralbio.2007.07.001>

59. Rombouts C, Giraud T, Jeanneau C, About I (2017) Pulp vascularization during tooth development, regeneration, and therapy. *Dent Res* 96:137–144. <https://doi.org/10.1177/0022034516671688>
60. Chmilewsky F, About I, Chung SH (2016) pulp fibroblasts control nerve regeneration through complement activation. *J Dent Res* 95:913–922. <https://doi.org/10.1177/0022034516643065>
61. Moss-Salentijn L, Applebaum E, Lammé AT (1972) Orofacial histology and embryology: a visual integration. F. A. Davis, Philadelphia, p xii 75 p. and slide set (180 col. slides. 182 × 182 in.)
62. Kucukkaya S, Gorduysus MO, Zeybek ND, Muftuoglu SF (2016) In Vitro Cytotoxicity of Calcium Silicate-Based Endodontic Cement as Root-End Filling Materials. *Scientifica* 2016:9203932. <https://doi.org/10.1155/2016/9203932>
63. Luo Z, Li D, Kohli MR, Yu Q, Kim S, He WX (2014) Effect of Biodentine on the proliferation, migration and adhesion of human dental pulp stem cells. *J Dent* 42:490–497. <https://doi.org/10.1016/j.jdent.2013.12.011>
64. Zanini M, Sautier JM, Berdal A, Simon S (2012) Biodentine induces immortalized murine pulp cell differentiation into odontoblast-like cells and stimulates biomineralization. *J Endod* 38:1220–1226. <https://doi.org/10.1016/j.joen.2012.04.018>
65. Erakovic M, Duka M, Bekic M, Tomic S, Ismaili B, Vucevic D, Colic M (2020) Anti-inflammatory and immunomodulatory effects of Biodentine on human periapical lesion cells in culture. *Int Endod J*. <https://doi.org/10.1111/iej.13351>

Publisher's note Springer Nature remains neutral with regard to jurisdictional claims in published maps and institutional affiliations.